PROCEEDINGS OF THE ROYAL SOCIETY B

Proc. R. Soc. B (2007) **274**, 1583–1589
doi:10.1098/rspb.2007.0328
Published online 24 April 2007

Optics of the ultraviolet reflecting scales of a jumping spider

Michael F. Land[1,*], Julia Horwood[1], Matthew L. M. Lim[2] and Daiqin Li[2]

[1]*Department of Biology and Environmental Science, University of Sussex, Brighton BN1 9QG, UK*
[2]*Department of Biological Sciences, National University of Singapore, 14 Science Drive 4, Singapore 117543, Republic of Singapore*

The jumping spider *Cosmophasis umbratica* from Singapore is strongly sexually dimorphic. The males, but not the females, reflect ultraviolet as well as green–orange light. The scales responsible for this are composed of a chitin–air–chitin sandwich in which the chitin layers are three-quarters of a wavelength thick and the air gap a quarter wavelength (where $\lambda = 600$ nm, the peak wavelength of the principal reflection maximum). It is shown that this configuration produces a second reflectance peak at approximately 385 nm, accounting for the observed reflection in the ultraviolet. Other scales have a similar thickness of chitin but lack the air gap and thus produce a dull purple reflection. This novel mechanism provides the spiders with two colour signals, both of which are important in mating displays.

Keywords: *Cosmophasis umbratica*; ultraviolet reflection; multilayer; structural colour; mating behaviour

1. INTRODUCTION

The jumping spider *Cosmophasis umbratica* is a highly ornamented species from Singapore (figure 1*a*) in which the two sexes are very different (Lim & Li 2004). They have an intriguing sexual recognition system that involves the use of ultraviolet (UV) by both sexes, but in very different ways. Many parts of the male's body are covered with scales that reflect in both the visible spectrum and the near-UV (figure 1*c*). Females reflect in the visible spectrum, though less brightly than males, but do not reflect ultraviolet (Lim & Li 2006*a*). During courtship, a male displays his reflecting parts in front of the female, and she will only accept a male that reflects in the UV. Females have palps that absorb UV and fluoresce green. Males show interest only in females with appropriately fluorescing palps (Lim *et al.* 2007).

In this paper, we investigate the mechanism responsible for the visible and ultraviolet reflection from the scales of the male. The most common way of producing a high reflectance from biological surfaces is by the use of thin-film multilayers (reviews Land 1972; Fox 1976; Herring 1994; Parker 2005). These structures are composed of several layers of alternating high and low refractive index material. In terrestrial insects such as iridescent butterflies, these are usually chitin (refractive index (n) = 1.5–1.6) and air ($n = 1$). The structures involved in insect scales can be very elaborate (Ghiradella 1998), but the specular (mirror-like) reflectors always consist of alternating layers with a sub-micrometre periodicity (Vukusic 2005). A high reflectance is achieved when light reflected from every interface in a stack emerges in phase, and the condition for this is that each layer in the stack should have an optical thickness (thickness × refractive index) of a quarter wavelength, or an odd multiple of this. This means that for quarter-wavelength reflectors the layers must be very thin, in the range 50–150 nm.

* Author for correspondence (m.f.land@sussex.ac.uk).

Electronic supplementary material is available at http://dx.doi.org/10.1098/rspb.2007.0328 or via http://www.journals.royalsoc.ac.uk.

Ultraviolet coloration and ultraviolet photoreception are now known to be common in the animal kingdom, particularly in insects and birds (Tovée 1995). In certain pierid butterflies, the UV reflectance is produced from a stack of quarter-wave cuticular lamellae with air spaces between them, protruding laterally from each scale ridge. In *Eurema lisa*, there are eight such layer pairs, with 55 nm thick lamellae and 83 nm spaces between them. These would give a peak reflectance at 343 nm, close to the measured peak at 348 nm (Ghiradella *et al.* 1972). *Colias eurytheme* also has a very similar structure (Kemp *et al.* 2006). However, it is clear that a simple quarter-wavelength stack will not produce the kind of reflection we find in male *C. umbratica*. If such a multilayer were to produce a peak reflectance in the visible spectrum, then that peak would be much broader than that observed here (figure 1*c*, see also figure 4*a*), and there would be no secondary peak in the near-UV. Making one layer of each pair thicker and the other thinner (so that the combination still has an optical thickness of half a wavelength) would narrow the visible peak somewhat and also introduce a peak in the far-UV (Land 1972, fig. 9). However, this peak would be at 300 nm or less, not close to the near-UV peak at approximately 385 nm observed here. An earlier electron microscope study of iridescent scales in the jumping spider *Corythalia canosa* indicated a structure of upper and lower chitin plates, each less than a micrometre thick, with a narrow space between them (Townsend & Felgenhauer 1999). Our results, from electron microscopy, interference microscopy and optical modelling, confirm that *C. umbratica* scales are similar. We show that the scales have a novel optical structure consisting of a 3/4–1/4–3/4 wavelength chitin–air–chitin sandwich. This does produce a reflectance spectrum (figure 4*b*) closely resembling that in figure 1*c*.

2. MATERIAL AND METHODS

(a) *Animals*

Cosmophasis umbratica were collected from open vegetation in Singapore. Reflectance measurements of different parts of the

Received 8 March 2007
Accepted 2 April 2007

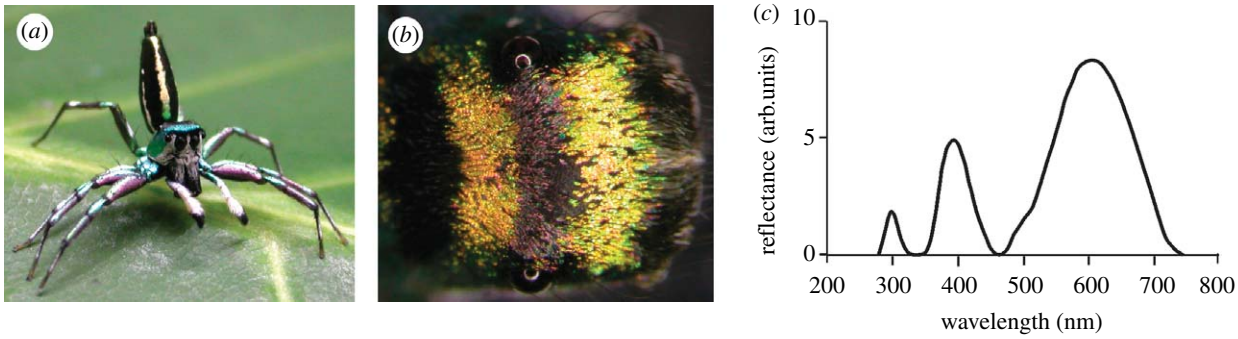

Figure 1. (*a*) Male *C. umbratica* in courting posture. The spiders are approximately 7 mm long. (*b*) Dorsal view of cephalothorax, facing right, showing two bars of green–orange reflecting scales with dull purple scales between them. (*c*) Reflectance spectrum of green–orange region.

body were made on live, recently collected animals, as described by Lim & Li (2006*a*). Those parts used for microscopy and interference measurements were preserved in 70% alcohol and sent to the UK. In alcohol, the normally green–orange regions were a dull purple colour, but on drying out the original colours were fully restored, implying that in life the scales are dry structures.

(b) *Light and electron microscopy*

A small piece of cuticle containing both type I (green–orange reflecting) and type II (dull purple) scales was cut from the dorsal cephalothorax (figure 1*b*). This was washed in buffer (0.2 M sucrose in 0.075 M sodium cacodylate, pH 7.4) and placed in 1% osmium tetroxide in 0.075 M sodium cacodylate buffer for an hour. It was washed in buffer and placed in a saturated solution of uranyl acetate for 30 min, washed again in buffer and then dehydrated through an ascending series of alcohol concentrations. It was washed three times in propylene oxide and left in a 50 : 50 mixture of propylene oxide and Spurr's resin on a rotator overnight, then placed in fresh resin and infiltrated for a week, with the resin changed every 2 days. The sample was embedded in fresh resin and polymerized at 60°C overnight.

The block was trimmed roughly and cut using an LKB Ultratome III. Two-micrometre-thick light microscope sections were cut with a dry glass knife, cover-slipped using Histomount and photographed unstained using a Zeiss Axiophot microscope with a 100× oil immersion lens. Once an area of interest was found, the block was trimmed for EM and ultrathin (60–120 nm) sections were obtained using a diamond knife. Grids were stained with Reynolds lead citrate and then viewed using a Hitachi 7100 transmission electron microscope (100 kV acceleration voltage) with an axially mounted Gatan Ultrascan 1000 CCD camera.

(c) *Interference microscopy*

The path differences between individual scales and two media, air ($n=1$) and immersion oil ($n=1.516$), were measured using a Vickers M41 interference microscope of the double-refracting Baker type. In the microscope, the condenser splits the illuminating beam into two via a calcite plate. One beam passes through the specimen and the other through the medium, and when the beams are recombined in the objective they interfere so that path differences show up as differences in interference colour or as differences in intensity when using monochromatic light ($\lambda=549$ nm). The measurement is made using a polarizing compensator which can be rotated so that either the specimen or the background adopts a particular interference colour. With monochromatic light, the most sensitive measurement is made by adjusting to give the darkest intensity. The difference in compensator readings then gives the angular phase difference between specimen and background, which can be converted to a path difference by multiplying with the wavelength used. When 10 pairs of measurements are made, the standard error of the path difference is 3 nm.

The path difference (pd) is the difference in optical thickness (thickness $d\times$refractive index n) between specimen (s) and medium (m), i.e. dn_s-dn_m, or $d(n_s-n_m)$. When path differences are measured for the same scales in air and immersion oil, two values are obtained,

$$\mathrm{pd}_{air}=d(n_s-1), \qquad \mathrm{pd}_{oil}=d(n_s-1.516),$$

from which the refractive index n_s and specimen thickness d can be obtained by solving the simultaneous equations

$$n_s=\frac{(1.516\mathrm{pd}_{air}-\mathrm{pd}_{oil})}{(\mathrm{pd}_{air}-\mathrm{pd}_{oil})}, \qquad d=\frac{(\mathrm{pd}_{air}-\mathrm{pd}_{oil})}{0.516},$$

where the structure is not homogeneous (for example if it is a multilayer) the values of n_s and d must be treated with caution, because they apply the combination of media.

(d) *Reflectance measurements*

Reflectance measurements on single scales were made using an Ocean Optics USB2000 spectrometer in combination with a microscope that could be used in either epi or transmission mode (figure 2). Using a 40× objective, single scales were imaged onto the tip of the 4 mm light guide of the instrument, and the field iris was stopped down to confine the illumination to a single scale. The background of the slide without the scale was used as the reference illuminant. Reflectance measurements were made without a cover-slip to avoid unwanted reflections.

3. RESULTS

(a) *Microscopical appearance and structure*

Many parts of the male's body are iridescent (figure 1*a*). The cephalothorax, abdomen and legs all reflect both visible (green to orange) and near-ultraviolet wavelengths. On the palps and clypeus, the reflectance is whiter, without clear peaks, although the reflectance still extends into the ultraviolet. Full-spectrum reflectance measurements made in air at near normal incidence from the brightly iridescent part of the cephalothorax (figure 1*b*) show a pattern of clearly defined peaks (Lim & Li 2006*a*). The largest is centred near 600 nm and has a width at half

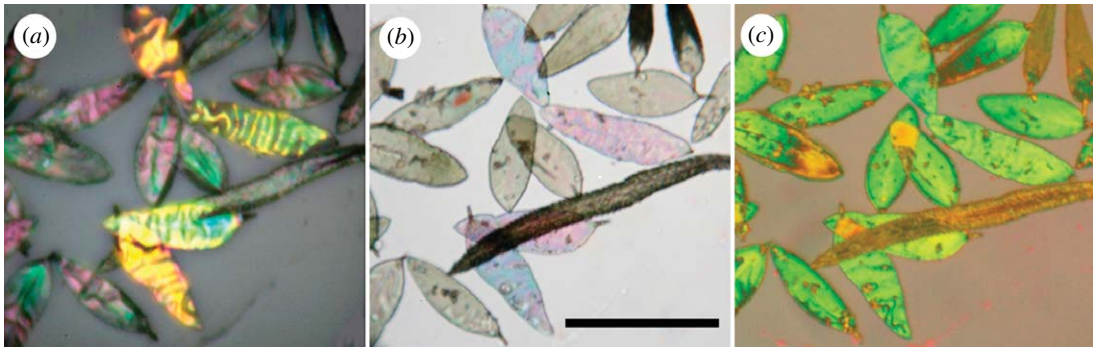

Figure 2. Micrographs of the same scales from the dorsal cephalothorax of *C. umbratica* using different techniques. (*a*) Epi-illumination, showing four highly green–orange reflecting (type I) scales and a number of weakly purple-reflecting type II scales. (*b*) Transmission micrograph. The type I scales that reflected green transmit unsaturated purple and the more orange scales transmit blue. Type II scales are almost colourless or weakly green. Scale bar, 100 μm. (*c*) Interference micrograph of scales in air. The consistency of the interference colour shows that all the scales have very similar path differences in air, indicating a similar thickness of chitin (table 1). Where scales overlap, the path difference doubles and the interference colour changes. Pigmented scales appear brown.

height (half-width) of 160 nm (figure 1*c*). It is this peak that gives the region its visible iridescent appearance. There is a second smaller peak in the violet/near ultraviolet region centred just below 400 nm with a half-width of 60 nm, and a small and variable third peak close to 300 nm in the far ultraviolet. The absolute value of the reflectance is hard to determine from the measurements of the whole carapace, because the reflection is neither diffuse nor specular, but disperses a collimated beam over about a 90° angle.

There are several types of scales on the cephalothorax of *C. umbratica*, but the two of particular interest here are the type I scales which strongly reflect green–orange light and weakly transmit purple, and the morphologically similar type II which weakly reflect various colours and are almost colourless in transmitted light (figure 2). The type I scales are strongly corrugated (figures 2*a* and 3*a*) and the type II less so. The function of the corrugations is presumably to increase the angle over which the bright reflection is visible. A third type of scale, shown in figure 2, is long, thin and heavily pigmented.

Reflectance measurements of single scales showed that the type I scales had peak reflectances between 540 and 620 nm, and these peaks had a half-width of approximately 140 nm. Unfortunately, the optics of the microscope did not permit measurements below 410 nm, but all scales showed a rise in reflectance below 450 nm, consistent with the presence of a near-UV peak, as in figure 1*c*. The type II scales had much lower reflectance peaks at approximately 650 and 470 nm, and a minimum at 560 nm.

The absolute value of the peak reflectance cannot be easily determined owing to the spread of reflected light caused by the corrugations in the surface. However, the absolute reflectance could be estimated from the transmittance since there is little, if any, absorption in these scales, and unlike the reflected light the transmitted light is not dispersed. The transmittance curves for type I scales had, as expected, a shape that was almost the inverse of the reflectance curves. For seven scales, the absolute difference between the maximum (approx. 600 nm) and the minimum (approx. 470 nm) varied between 18 and 47%, with a mean of 30%. This also implies that the maximum reflectance has a similar absolute value of approximately 30%. In the type II scales, the highest

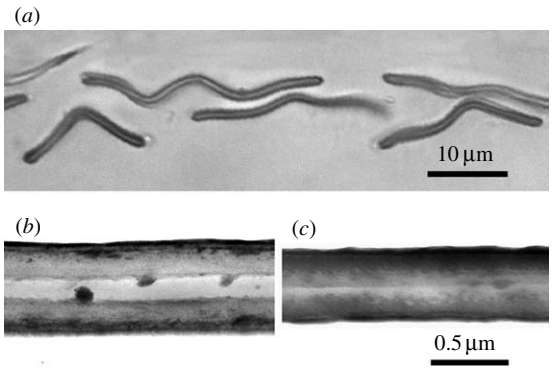

Figure 3. (*a*) Light micrograph of an unstained section through several type I scales, showing the sandwich-like structure, and the undulating appearance. 100× oil immersion. (*b*) Electron micrograph of a section of a type I scale showing the sandwich structure. (*c*) Section through a type II scale showing a solid structure with a central line dividing the two halves.

observed transmittance difference between maxima and minima was approximately 15%.

Two-micrometre-thick resin sections of the scales (figure 3*a*) showed that the yellow–green reflecting scales were extremely thin (less than 1 μm) and had a sandwich structure, with two thicker layers and a thin layer of optically different composition between them. At the outer edges of the scale, the cavity appeared to be closed, indicating that the contents are not open to the outside. Most scales had undulations, consistent with the corrugations in figure 2*a*. Other scales, which we assume to be the weakly reflecting type II scales, lacked the middle layer and appeared solid.

Transmission electron micrographs confirmed the structures seen in the light micrographs (figure 3*b*,*c*). Type I scales have a sandwich structure. The outer layers are not completely uniform, but stain more densely towards the outside. The cavity is parallel sided and hollow except for irregular ball-like outgrowths from the walls. These have not been seen to join up across the cavity to form bridges or pillars, but they may nevertheless serve to keep the cavity open. The width of the cavity varied somewhat, probably due to the processing procedures, but typical widths were 0.13 μm for the cavity and 0.24 μm for the

Table 1. Interference microscope measurements of five green–orange reflecting (type I) and five dull purple (type II) scales. (Measurements in nm.)

measurement	type I	type II
path difference (air) $= d(n_s - 1)$	322.8 ± 9.6 (s.d.)	293.6 ± 9.4 (s.d.)
path difference (oil) $= d(n_s - 1.516)$	27.2 ± 4.2	34.4 ± 4.7
thickness $d = (pd_{air} - pd_{oil})/0.516$	572.9 ± 22.3	502.3 ± 19.9
$n_s = (1.516pd_{air} - pd_{oil})/(pd_{air} - pd_{oil})$	1.564 ± 0.008	1.584 ± 0.011

walls (0.61 μm overall). The type II scales were solid, with a typical width of 0.46 μm. In nearly all sections there is a definite junction down the centre of the scale (figure 3*c*), leading to the suggestion that scales are formed of two halves, somewhat like the type I scales but without the gap.

(b) *Interference microscopy*

Under interference microscopy, both type I and type II scales have very similar path differences in air, in the range 270–340 nm (figure 2*c*). Assuming that they are made principally of chitin, this implies that they both have a similar total thickness of chitin. The path differences, calculated thicknesses and refractive indices for five scales of each type are given in table 1.

In interpreting these figures, it is important to recall that the type I scales are highly reflecting because they have a gap, presumed to be air, between the chitin layers, and that the type II scales are dull because they have no such gap. A consequence of this is that the apparent refractive index for the type I scales will be reduced somewhat owing to that gap. (We assume here that the closed nature of the gap prevents oil from replacing the air. This is confirmed by the observation that the type I scales still reflect light when they are immersed in oil.) The difference in measured refractive index between type I and type II scales is significant *t*-test: $p < 0.02$, but the variance is too large for this difference to be used to estimate accurately the width of the air gap in the type I scales. Since the type II scales are solid, their refractive index (1.584) is likely to be closest to the true value for chitin.

Using this value (1.584) and the path difference in air for the type I scales, we can calculate the actual thickness of chitin in the type I scales. Since the medium both outside and in the gap in the scales is air, the path difference in air should give the true thickness of the chitin alone. This thickness is then $pd_{air}/(n_{chitin} - 1)$, i.e. $322.8/0.584 = 552.7$ nm. If we make the further assumption that this is divided equally between two layers, as the microscopy suggests, then each has a thickness of 276.4 nm. Multiplying this by the refractive index of chitin (1.584) gives each layer an optical thickness (nd) of 437.8 nm. The significance of this is that it is three-quarters of 583.7 nm, which is well within the range of wavelengths that the scales reflect best (540–620 nm). Since maximum constructive interference occurs when the optical thickness of a plate is an odd multiple of a quarter wavelength, these plates appear to be the right thickness to produce a high reflectance, especially if the air gap between them also has an optical thickness of a quarter wavelength, or an odd multiple of that (§3*c*).

The thickness measurements obtained from electron microscopy (figure 3) are 10–15% lower than those from interference microscopy (which should be the more accurate method), but this is consistent with the expected shrinkage from the method of preparation.

(c) *Optical modelling*

It was expected that the three layers of the chitin–air–chitin sandwich structures of the type I scales would all have optical thicknesses close to odd multiples of $\lambda/4$, i.e. approximately 150 nm if λ is 600 nm. Such structures give the greatest constructive interference and hence the highest reflectance at λ. The spectral reflectance of multilayer structures can be determined by standard methods (e.g. Vašiček 1960), but a particularly convenient method has been provided by Huxley (1968, p. 241; see electronic supplementary material), which was used here in a MATLAB program. The three plausible configurations are chitin–air–chitin structures where the optical thicknesses of the layers are $\lambda/4$–$\lambda/4$–$\lambda/4$, $3\lambda/4$–$\lambda/4$–$3\lambda/4$ and $3\lambda/4$–$3\lambda/4$–$3\lambda/4$, where $\lambda = 600$ nm. The results of the reflectance calculations are shown in figure 4, and it is clear that a very good fit to the measured data in figure 1*c* is given by the $3\lambda/4$–$\lambda/4$–$3\lambda/4$ structure (figure 4*b*). Both theoretical and measured spectra have three peaks of ascending magnitude and increasing width at around 320, 385 and 600 nm, with troughs of zero reflectance between them. In the $\lambda/4$–$\lambda/4$–$\lambda/4$ structure, the main peak is much too broad, with a half-width of more than 400 nm (figure 4*a*), and it can be ruled out. The $3\lambda/4$–$3\lambda/4$–$3\lambda/4$ structure gives a somewhat better fit, but the gap between the visible and UV peaks is much larger than that measured on either the intact animal or single scales (figure 4*c*). The main peak is narrower than in the data (half-width 115 nm compared with measured values between 140 and 160 nm). Finally, the UV and visible peaks have equal heights in the $3\lambda/4$–$3\lambda/4$–$3\lambda/4$ model, whereas in the data they are unequal. On all these counts, the $3\lambda/4$–$\lambda/4$–$3\lambda/4$ model gives the best fit. This structure is also the one most consistent with the anatomical measurements. Note that other combinations do not produce peaks at appropriate wavelengths: for example a $3\lambda/4$–$\lambda/2$–$3\lambda/4$ structure has a reflectance *minimum* at 600 nm.

The only important discrepancy between the reflectance of the $3\lambda/4$–$\lambda/4$–$3\lambda/4$ model and the measured data is in the magnitude of the reflectance. The single-scale transmittance data suggest that in real scales, the peak reflectance is approximately 30%, as opposed to 53% in the model. Various kinds of imperfection might reduce reflectance, but one possible cause is the presence of the irregular structures in the air gap, seen in figure 3*b*, which might have the effect of increasing the effective refractive index of the gap. Thus, if the effective refractive index of the gap is increased from 1.0 to 1.1, then the peak reflectance falls to 39%, and with an increase to 1.2, it falls to 20%. The shape of the reflectance curve is not affected by these refractive index changes. There is also the

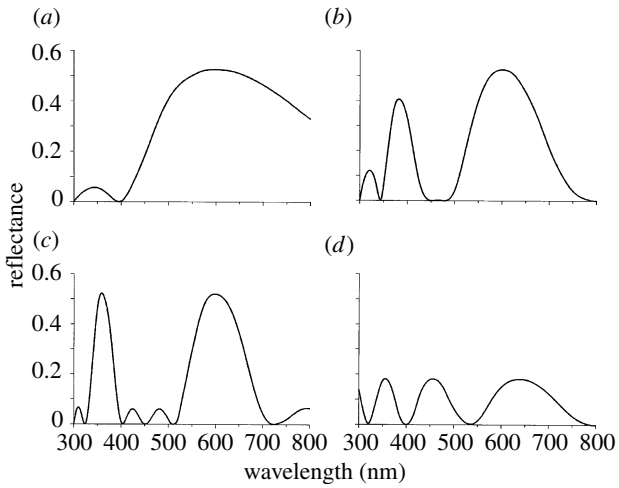

Figure 4. (*a–c*) Theoretical spectral reflectance of three-layer, chitin–air–chitin multilayers, in which the optical thicknesses are multiples of a quarter wavelength ($\lambda = 600$ nm). The configurations of the layers are (*a*) $\lambda/4$–$\lambda/4$–$\lambda/4$, (*b*) $3\lambda/4$–$\lambda/4$–$3\lambda/4$ and (*c*) $3\lambda/4$–$3\lambda/4$–$3\lambda/4$. (*d*) Spectral reflectance of a single chitin plate of optical thickness 800 nm.

possibility that there is some absorption by the scales, but this cannot be great as the scales are nearly invisible by transmitted light when in immersion oil.

A feature that does affect the balance between the visible and UV peaks is the thickness of the air gap. Decreasing it below 150 nm ($\lambda/4$) (and correspondingly increasing the thickness of the chitin layers to maintain the reflectance peak at 600 nm) increases the relative height of the near-UV peak (385 nm), and increasing the air gap thickness above $\lambda/4$ decreases it. There is thus some scope for fine-tuning the relative amounts of UV and visible light that are reflected. Small changes in gap thickness have minimal effects on the absolute reflectance at 600 nm. There is a second far-UV peak at 280 nm (not shown in figure 4*b*), and it is possibly the combination of this with the 320 nm peak that gives the small peak at 300 nm in the reflection from the cephalothorax (figure 1*c*).

Figure 4*d* shows the spectral reflectance for a homogeneous film of optical thickness 800 nm, modelling a type II scale with a thickness of 505 nm and a refractive index of 1.584 (table 1). It has peak reflectances of 18% at 640, 457 and 356 nm, consistent with a weak purple reflection in the visible spectrum.

4. DISCUSSION

(a) *Model of a type I scale*

Evidence from light and electron microscopy indicated that the highly reflecting scales of the cephalothorax are three-layer sandwich structures. The sandwich in this case almost certainly has a central layer of air, because air provides the lowest available refractive index in relation to the high-index chitin, and hence the highest reflectance at each interface. There is also little else that it could be, given that scales retain their optical properties when dry. Interference microscopy showed that the total thickness of the outer chitin layers in the sandwich was approximately 553 nm and the refractive index 1.584. This gives an optical thickness (nd) of 438 nm for each chitin layer, which is close to three-quarters of the visible wavelength that is best reflected (approx. 600 nm). Optical modelling

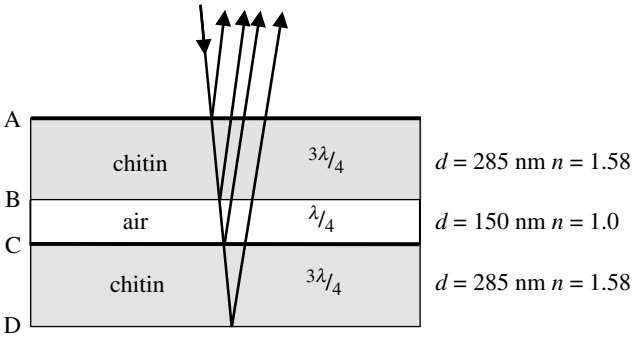

Figure 5. Model of a type I scale which reflects strongly at 600 nm, showing the materials, optical thicknesses as fractions of the peak wavelength, physical thicknesses (d) and refractive indices (n). Interfaces (A–D) are referred to in the text. Interfaces with heavy lines produce a $\lambda/2$ phase change. Type II scales have a similar structure but without the air layer.

(figure 4) indicated that a $3\lambda/4$–$\lambda/4$–$3\lambda/4$ chitin–air–chitin structure produced a reflectance spectrum that was very similar to the reflectance spectrum measured directly from the dorsal cephalothorax (figure 1*c*) as well as from the isolated scales. A study of the effects of varying the width of the air layer indicated that, from the relative heights of the visible and near-UV peaks in the spectrum, this layer must be close to or slightly thicker than 150 nm ($\lambda/4$).

A three-layer model consistent with all the above evidence is presented in figure 5. This model generates the spectral reflectance curve shown in figure 4*b*, which is very similar to the measured reflectance of the dorsal cephalothorax shown in figure 1*c*. Besides the principal reflectance peak at 600 nm, the model also generates a somewhat lower peak in the near ultraviolet at 385 nm. It seems that it is this near-UV peak that makes males attractive to conspecific females (Lim *et al.* 2007) and induces agonistic posturing between males (Lim & Li 2006*b*). Multilayer reflectors with this simple three-layer structure have been observed once before, in the wing scales of a butterfly *Papilio nireus* (Vukusic & Hooper 2005), but there the layers all have thicknesses close to a quarter wavelength.

(b) *The cause of the near-UV reflection peak*

A high reflectance occurs when light reflected from different interfaces interferes constructively. Light reflected from a low-to-high refractive index interface undergoes a $\lambda/2$ phase change, but this does not happen at high-to-low interfaces (e.g. Jenkins & White 1981, p. 288). This means that light reflected from the lower (non-retarding) surface of a high-index plate must undergo a $\lambda/2$ retardation as it passes twice through plate, if it is to emerge in phase with the light reflected from the upper (retarding) surface. This means that the plate must have an optical thickness of $\lambda/4$, or an odd multiple of $\lambda/4$. Plates (or spaces) with an optical thickness of $\lambda/2$, or multiples of $\lambda/2$, give destructive interference and will appear dark for the same value of λ.

In the case of a $3\lambda/4$–$\lambda/4$–$3\lambda/4$ sandwich, light reflected from all four interfaces interferes constructively; in this case, when $\lambda \sim 600$ nm. However, it is not so easy to provide a simple explanation for the peak at 385 nm. It will help to break down the structure into pairs of interfaces. Consider first interfaces A & B and C & D (figure 5). These give plates with an optical thickness of 450 nm and with one $\lambda/2$ retarding surface each. Thus, these will support a series of wavelengths, the longest of

which is 450×4 (1800) nm, then 450×4/3 (600) nm, 450×4/5 (360) nm, 450×4/7 (257) nm, etc. Now, consider interfaces A & C and B & D. These are separated by 600 nm and since both are low-to-high refractive index interfaces, no phase differences result and the supported wavelengths are the even multiples of 600×4 nm. The longest is 600×4/2 (1200) nm, then 600×4/4 (600) nm, 600×4/6 (400) nm, 600×4/8 (300) nm, etc. Interfaces B & C with a 150 nm gap support only 600 nm and then 150×4/3 (200) nm, etc. Interfaces A & D give a total optical thickness of 1050 nm. Applying the same logic, they should support the wavelength series 4200, 1400, 840, 600, 467, 382, 323 and 280 nm. Thus, all pairs of interfaces support constructive interference at 600 nm, and all except B & C (the air gap) also provide constructive interference close to 385 nm, i.e. at 360, 400 and 382 nm. It thus seems that the peak at 385 nm is a compromise between the contributions of light from different interfaces, with no one pair providing an exact match. This is why the 385 nm peak is lower than the 600 nm peak. In the model in which all layers are $3\lambda/4$ thick (figure 4*c*), there is complete constructive interference at 360 nm and the reflectance peak is of same height as the 600 nm peak.

(c) *Variations in structure and spectral reflectance*

The colours of the type I scales on different parts of the male spider's body vary slightly in visible colour, in the range from green to orange, with peak reflectances in the range 540–620 nm. This is most easily explained with the assumption that the chitin layers, or the air layer, or both, vary in thickness by approximately 25%. Varying the thickness of the air gap can also change the relative proportions of UV and visible light reflected, with thinner air gaps favouring the UV component. Another cause of apparent variation is the angle at which the scales are viewed. A property of all multilayer reflectors is that as the angle of viewing becomes shallower (away from the normal), the reflected colour shifts to shorter wavelengths, for example, orange becomes green. Such shifts are easily observed when rotating the spider under directional illumination.

The change from bright green–orange to dull purple or near black on the cephalothorax (figure 1*b*) appears to be accomplished very simply, by leaving out the air gap in the type II scales, without changing the total thickness of the chitin. This has the effect of reducing the four reflecting surfaces to two, decreasing the scope for constructive interference and hence the reflectance (figure 4*d*).

The scales on the palps of the male are different from those of the rest of the body. The outer regions reflect a purple colour rather weakly, presumably from a single layer in the same way as the type II scales from the cephalothorax. However, the heavily sculpted part near the spine of the scale reflects a diffuse white, presumably as a result of scattering by the numerous projections. Both regions will reflect some UV either by thin-film reflection (cf. figure 4*d*) or by spectrally non-specific scattering.

(d) *Colour and spider vision*

In salticids, the ability to resolve light of different wavelengths appears to be confined to the forward-pointing principal eyes. These have excellent resolution, a complex repertoire of retinal movements and are concerned with pattern recognition during courtship and prey capture (Forster 1985; Land 1985). The side eyes have lower resolution, receptors of only one spectral class (green sensitive; Blest *et al.* 1981) and are responsible mainly for the detection of moving objects. It has been known since 1975 that the principal eyes of jumping spiders have receptors that respond to green (peak near 530 nm) and UV light (peak 365–380 nm) (DeVoe 1975; Blest *et al.* 1981; Peaslea & Wilson 1989). Suggestions that there may also be blue–green (480–500 nm) and yellow (580 nm) sensitive receptors (Yamashita & Tateda 1976) have not so far been confirmed. When trained on a heat avoidance task, jumping spiders can learn to distinguish a range of colours from blue to red, both from one another, and from black, white and grey (Nakamura & Yamashita 2000). However, the relative contributions of hue and brightness are uncertain. Compelling evidence for the importance of colour for salticids comes from the coloured adornments on the parts of jumping spiders that are displayed during courtship, usually by males to females. Crane (1949) for example showed that the yellow patches on the clypeus of *Corythalia xanthopa* were essential for eliciting threat display. Even crude models with similar patches were effective, whereas models with white patches were not. None of this demonstrates true colour vision, in the sense of being able to recognize intermediate hues by comparing outputs of different receptor types, but it is certain that salticids have the ability to discriminate different wavelength ranges.

In a previous paper (Lim *et al.* 2007), we showed that in *C. umbratica*, the UV reflections from the legs and body of the males were crucial for inducing the characteristic courtship posture of the females. Conversely, it is the green colour of the female, enhanced by the UV-induced green fluorescence of the palps, that is required for the initiation and maintenance of the male's courtship display. Males confront each other (or their image in a mirror) with an agonistic display when UV light is present, but in the absence of UV light this may change to a courtship display (Lim & Li 2006). It thus appears that in *C. umbratica*, there are important roles for both major classes of photoreceptor in the principal eyes during courtship, although there is an intriguing sex difference in the way that UV and green coloration are interpreted.

So far, the only other report of UV perception in a jumping spider has been in the detection of the stabilimentum threads in the webs of the orb-web spider *Argiope versicolor* (Li & Lim 2005) by *Portia labiata*. *Portia* is a web-invading spider-eating salticid which preys on *Argiope* and uses the UV reflection from the stabilimentum threads (whose function, ironically, is to deter birds) to detect and discriminate between webs. Since UV receptors are ubiquitous among salticids, it seems likely that other functions will be found.

We thank the Singapore National Parks Board for research permit NR/RP104. This work was partially supported by grant R-154-000-140-112 to D.L. from the National University of Singapore Academic Research Fund. We thank Daniel Osorio (Sussex) for his help with single-scale spectrometry, and Peter Vukusic (Exeter), for comments on an earlier draft of the manuscript.

REFERENCES

Blest, A. D., Hardie, R. C., McIntyre, P. & Williams, D. S. 1981 The spectral sensitivities of identified receptors and

the function of the retinal tiering in the principal eyes of a jumping spider. *J. Comp. Physiol.* **145**, 227–239. (doi:10.1007/BF00605035)

Crane, J. 1949 Comparative biology of jumping spiders at Rancho Grande, Venezuela. Part IV. An analysis of display. *Zoologica* **34**, 159–214.

DeVoe, R. D. 1975 Ultraviolet and green receptors in principal eyes of jumping spiders. *J. Gen. Physiol.* **66**, 193–207. (doi:10.1085/jgp.66.2.193)

Forster, L. 1985 Target discrimination in jumping spiders (Araneae; Salticidae). In *Neurobiology of arachnids* (ed. F. G. Barth), pp. 249–274. Berlin, Germany: Springer.

Fox, D. L. 1976 *Animal biochromes and structural colours*. Berkeley, CA: University of California Press.

Ghiradella, H. 1998 Hairs, bristles and scales. In *Microscopic anatomy of invertebrates*, vol. 11A (ed. M. Locke) Insecta, pp. 257–287. New York, NY: Wiley.

Ghiradella, H., Aneshansley, D., Eisner, T., Silberglied, R. E. & Hinton, H. E. 1972 Ultraviolet reflection of a male butterfly: interference colour produced by thin-layer elaboration of wing scales. *Science* **178**, 1214–1217. (doi:10.1126/science.178.4066.1214)

Herring, P. J. 1994 Reflective systems in aquatic animals. *Comp. Biochem. Physiol. A* **109**, 513–546. (doi:10.1016/0300-9629(94)90192-9)

Huxley, A. F. 1968 A theoretical treatment of the reflexion of light by multilayer structures. *J. Exp. Biol.* **48**, 227–245.

Jenkins, F. A. & White, H. E. 1981 *Fundamentals of optics*, 4th edn. Singapore: McGraw-Hill.

Kemp, D. J., Vukusic, P. & Rutowski, R. L. 2006 Stress-mediated covariance between nano-structured architecture and ultraviolet butterfly coloration. *Funct. Ecol.* **20**, 282–289. (doi:10.1111/j.1365-2435.2006.01100.x)

Land, M. F. 1972 The physics and biology of animal reflectors. *Prog. Biophys. Mol. Biol.* **24**, 75–106. (doi:10.1016/0079-6107(72)90004-1)

Land, M. F. 1985 The morphology and optics of spider eyes. In *Neurobiology of arachnids* (ed. F. G. Barth), pp. 53–78. Berlin, Germany: Springer.

Li, D. & Lim, M. L. M. 2005 Ultraviolet cues affect the foraging behaviour of jumping spiders. *Anim. Behav.* **70**, 771–776. (doi:10.1016/j.anbehav.2004.12.021)

Lim, M. L. M. & Li, D. 2004 Courtship and male–male agonistic behaviour of *Cosmophasis umbratica* Simon, an ornate jumping spider (Araneae: Salticidae) from Singapore. *Raffles Bull. Zool.* **52**, 435–448.

Lim, M. L. M. & Li, D. 2006*a* Extreme ultraviolet sexual dimorphism in jumping spiders (Araneae: Salticidae). *Biol. J. Linn. Soc.* **89**, 397–406. (doi:10.1111/j.1095-8312.2006.00704.x)

Lim, M. L. M. & Li, D. 2006*b* Behavioural evidence of UV sensitivity in jumping spiders (Araneae: Salticidae). *J. Comp. Physiol. A* **192**, 871–878. (doi:10.1007/s00359-006-0126-5)

Lim, M. L. M., Land, M. F. & Li, D. 2007 Sex-specific UV and fluorescence function as courtship signals in jumping spiders. *Science* **315**, 481. (doi:10.1126/science.1134254)

Nakamura, T. & Yamashita, N. 2000 Learning and discrimination of coloured papers in jumping spiders (Araneae, Salticidae). *J. Comp. Physiol. A* **186**, 897–901.

Parker, A. R. 2005 'Simple' classical optics in animals—reflectors and anti-reflectors. In *Structural colors in biological systems* (eds S. Kinoshita & S. Yoshioka), pp. 29–52. Osaka, Japan: Osaka University Press.

Peaslea, A. G. & Wilson, D. 1989 Spectral sensitivity in jumping spiders (Araneae, Salticidae). *J. Comp. Physiol. A* **164**, 359–363. (doi:10.1007/BF00612995)

Tovée, M. J. 1995 Ultraviolet photoreceptors in the animal kingdom: their distribution and function. *Trends Ecol. Evol.* **10**, 455–460. (doi:10.1016/S0169-5347(00)89179-X)

Townsend, V. R. & Felgenhauer, B. E. 1999 Ultrastructure of the cuticular scales of lynx spiders (Araneae: Oxyopidae) and jumping spiders (Araneae: Salticidae). *J. Morphol.* **240**, 77–92. (doi:10.1002/(SICI)1097-4687(199904)240:1<77::AID-JMOR6>3.0.CO;2-P)

Vašiček, A. 1960 *Optics of thin films*. Amsterdam, The Netherlands: North-Holland.

Vukusic, P. 2005 Structural colour effects in Lepidoptera. In *Structural colors in biological systems* (eds S. Kinoshita & S. Yoshioka), pp. 95–112. Osaka, Japan: Osaka University Press.

Vukusic, P. & Hooper, I. 2005 Directionally controlled fluorescence emission in butterflies. *Science* **310**, 1151. (doi:10.1126/science.1116612)

Yamashita, S. & Tateda, H. 1976 Spectral sensitivities of jumping spider eyes. *J. Comp. Physiol. A* **105**, 29–41. (doi:10.1007/BF01380051)